A dynamic multi-agent approach for modeling the evolution of multi-hazard accident scenarios in chemical plants

Chen, Chao; Reniers, Genserik; Khakzad, Nima

DOI
10.1016/j.ress.2020.107349

Publication date
2020

Document Version
Final published version

Published in
Reliability Engineering and System Safety

Citation (APA)
Chen, C., Reniers, G., & Khakzad, N. (2020). A dynamic multi-agent approach for modeling the evolution of multi-hazard accident scenarios in chemical plants. *Reliability Engineering and System Safety*, *207*, Article 107349. https://doi.org/10.1016/j.ress.2020.107349

Reliability Engineering and System Safety 207 (2021) 107349

Contents lists available at ScienceDirect

Reliability Engineering and System Safety

journal homepage: www.elsevier.com/locate/ress

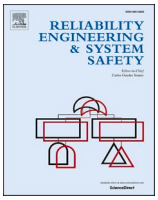

A dynamic multi-agent approach for modeling the evolution of multi-hazard accident scenarios in chemical plants

Chao Chen [a], Genserik Reniers [a,b,c,*], Nima Khakzad [d,*]

[a] Safety and Security Science Group, Faculty of Technology, Policy and Management, TU Delft, Delft, the Netherlands
[b] Faculty of Applied Economics, Antwerp Research Group on Safety and Security (ARGoSS), University Antwerp, Antwerp, Belgium
[c] CEDON, KULeuven, Campus Brussels, Brussels, Belgium
[d] School of Occupational and Public Health, Ryerson University, Toronto, Canada

ARTICLE INFO

Keywords:
Multi-hazard risk assessment
Toxic release
Cascading effects
Dynamic evolution
Multi-agent

ABSTRACT

In the chemical industry, multi-hazard (toxic, flammable, and explosive) materials such as acrylonitrile are stored, transported, and processed in large quantities. A release of multi-hazard materials can simultaneously or sequentially lead to acute toxicity, fire and explosion. The spatial-temporal evolution of hazards may also result in cascading effects. In this study, a dynamic methodology called "Dynamic Graph Monte Carlo" (DGMC) is developed to model the evolution of multi-hazard accident scenarios and assess the vulnerability of humans and installations exposed to such hazards. In the DGMC model, chemical plants are modeled as a multi-agent system with three kinds of agents: hazardous installations, ignition sources, and humans while considering the uncertainties and interdependencies among the agents and their impacts on the evolution of hazards and possible escalation effects. A case study is analyzed using the DGMC methodology, demonstrating that the risk can be underestimated if the spatial-temporal evolution of multi-hazard scenarios is neglected. Vapor cloud explosion (VCEs) may lead to more severe damage than fire, and the safety distances which are implemented only based on fire hazards are not sufficient to prevent from the damage of VCEs.

1. Introduction

The past decades have witnessed an increase in the number, size, and diversity of chemical plants due to the increasing population and the increasing requirement for products (energy, chemicals, commodities, and food, etc.) [1,2]. The rapid expansion of the process plants and infrastructures brings huge economic benefits while unavoidably increasing the exposure to major hazards caused by hazardous materials in chemical industrial areas, resulting in human losses, environmental damage and economic losses [3–7]. Major hazards such as fire, explosion, and toxic release arising from loss of containments may occur due to intentional or unintentional causes [8–11]. Intentional hazards are security-related threats, including terrorist attacks, sabotage, thief, etc. Unintentional hazards consist of accidental hazards (e.g., corrosion, fatigue, mechanical damage) and natural hazards (e.g., earthquake, flood, lightning). In hazardous chemical areas, fire is the most frequent hazard (44%), followed by explosion (36%). Toxic release without fire and explosion accounts for 20% of all major accidents and toxic substances are involved in almost 30% of these accidents [12]. Besides, chemical industrial areas are usually congested with hazardous storage tanks, complex piping, high-pressure compressors, and separators in which a loss of containment (LOC) event may lead to cascading effects and multiple hazards.

All the major hazards of fire, explosion and toxic release can be simultaneously or sequentially present in one disaster due to the evolution of hazards. Many catastrophic disasters in the past two decades originated from the hazardous release of process vessels and evolved to VCEs and finally fires. On October 23, 2009, a large VCE happened at the Caribbean Petroleum Corporation (CAPECO) terminal in Bayamón, Puerto Rico, during the offloading of gasoline from a tanker [13]. The subsequent fires triggered by the explosion lasted about 60 h and resulted in significant damage to 17 of the 48 petroleum storage tanks and other equipment [13]. On November 28, 2018, a Vinyl chloride release in a chemical plant at Zhangjiakou (China) caused a VCE outside the chemical plant, triggering fires on tank trucks and leading to 23 fatalities and 22 injuries [14].

In light of these past disasters and due to the severe consequences of unpredicted hazards, modeling the spatial-temporal evolution of

* Corresponding authors.
E-mail addresses: c.chen-1@tudelft.nl (C. Chen), g.l.l.m.e.reniers@tudelft.nl (G. Reniers), nima.khakzad@ryerson.ca (N. Khakzad).

https://doi.org/10.1016/j.ress.2020.107349
Received 18 June 2020; Received in revised form 6 October 2020; Accepted 9 October 2020
Available online 23 November 2020

hazards originating from release of hazardous materials in industrial areas is essential for protecting staff, nearby residents and emergency rescuers [15–17]. For example, in the Tianjin port disaster in 2015, which was caused by a spontaneous ignition of nitrocellulose, many of the emergency rescuers were killed in the disaster due to an unpredicted evolution of the fire to an explosion. Besides, the disasters caused by natural hazards (Na-tech) can make emergency response more difficult due to the damage to safety barriers and other infrastructures, resulting in more severe consequences [18–22]. To avoid such catastrophic disasters, many post-accident analyses have been conducted to predict the overpressure induced by explosions [23–27] and vapor cloud dispersion [28–30]. Besides, a lot of work has been done on vulnerability assessment of installations to VCEs, risk assessment of domino effects caused by VCE [31–36] and domino effects triggered by fire [37–39]. Regarding the evolution of fire, the time to failure of equipment exposed to fire is critical for assessing the vulnerability of installations. As a result, dynamic methods were used to assess the vulnerability of installations exposed to fire and fire-induced domino effects [40–44]. Among these dynamic tools, the dynamic graph approach and the dynamic Bayesian network approaches are able to model the spatial-temporal evolution of domino effects caused by fire and visualize the escalation paths of fire [8,11,40]. Monte Carlo simulation has also been applied to address the evolution uncertainty of domino effects [45].

Compared to the research devoted to VCE or fire evolution, little attention has been paid to the evolution of possible toxic release, VCE and fire in a catastrophic disaster and the assessment of human exposure to multiple hazards. Dai et al. [46] analyzed the vulnerability of tanks exposed to fire and explosion in different accidents, but overlooked the possible evolution between different hazards. He and Weng [47] studied the synergic effects of multi-hazard on vulnerability assessment but ignored the dynamic evolution process. The evolution of toxic release to VCE and vice versa is a dynamic process along with a vapor cloud dispersion [48]. The present study, therefore, aims to establish a dynamic methodology for human and facility vulnerability assessment considering the spatial-temporal evolution of multiple hazards: toxic release, VCE, and fire. In our study, chemical plants are modeled as a multi-agent (component) system [49,50] through the application of dynamic graphs. Graph-based methods have been used for domino effect analysis, vulnerability and reliability analysis, and resilience assessment. Besides, Monte Carlo simulation [51] is used in this study to solve the dynamic multi-agent model. Consequently, both the uncertainty of ignition and the uncertainty of evolution of different hazards are taken into consideration in the present study. The model and algorithm are developed in Section 2. A case study is provided in Section 3 to show the application of the developed methodology. A discussion based on the results of the case study is presented in Section 4. The conclusions of this study are summarized in Section 5.

2. Methodology

Graph-based methods are commonly used and are effective tools to analyze multiple interacting agents in a system [52,53]. In a graph, the agents are modeled by nodes and their dependencies are represented by edges [38,44,54]. As a result, graph-based methods provide a visible structure (graph or network) to represent the complex agent interactions while agent-based modeling focuses on agent behaviors (e.g., attributes and interactions), making it very flexible to model socio-technical systems [50,55,56]. Graph metrics such as betweenness and closeness have been used to assess domino effects and the vulnerability of installations subject to fire and explosion hazards [38,57]. The time-dependent escalation of fire can also be modeled by dynamic graphs [41]. The dynamic graph approach is able to model the dynamic evolution of fire hazard while static graph methods provide merely a snapshot of the whole process at once. When it comes to modeling the evolution between different hazards, it is difficult to address the uncertainty in hazard evolution by merely using the dynamic graph approach. Compared with analytical methods, Monte Carlo simulation is widely used to model uncertainties that cannot be easily accounted for due to the intervention of random variables, avoiding complex mathematical calculations [58–60]. In this study, a new methodology is developed based on dynamic graphs and Monte Carlo simulation to model the complexity and uncertainty of hazard evolution. The methodology is called Dynamic Graph Monte Carlo (DGMC). The DGMC is defined as a dynamic graph with time-dependent parameters and random parameters in which Monte Carlo simulation is used to solve the model.

2.1. Modeling

In order to model the hazard evolution process and thereby dynamically assess human vulnerability exposed to the possible toxic cloud, heat radiation, and overpressure, we define a Hazard Evolution Graph (HEG) based on the developed DGMC method. The HEG can be defined as a dynamic graph with nine-tuple, as shown in Eq. (1).

$$HEG = (T, M, N, K, S, E, C, P, H) \tag{1}$$

2.2.1. Evolution time

$T = [t_1, t_2, t_3, \ldots, t_G]$ represents the evolution time of hazards starting from a hazardous release (t_1=0). The dynamic graph *HEG* is sliced into G static graphs by these time nodes. The *HEG* parameters are updated at each time node t_g due to the change of hazards, human states, and installation states. If an ignition occurs, t_2 is equal to the ignition time (*IT*). *IT* is a random variable that depends on the number of ignition sources, ignition effectiveness, and vapor cloud dispersion, etc. The *IT* is equal to zero if the released materials are immediately ignited. In the chemical industry, the likelihood of immediate ignition is always determined by the autoignition of flammable substances and the static discharge caused by the release [48]. If the ignition is delayed, the possible ignitions caused by different ignition sources are considered as independent events, and the ignition probability of a single ignition source depends on the ignition effectiveness and the period that the ignition source is covered by the flammable vapor, as follows [61]:

$$f_{I,k} = 1 - e^{-\omega \times t_{I,k}} \tag{2}$$

$f_{I,k}$ represents the cumulative ignition probability caused by the ignition source k. ω denotes the ignition effectiveness of the ignition source. $t_{I,k}$ represents the time that ignition source k (within the flammability limit) is covered by the flammable vapor. To determine t_{IS}, the vapor cloud dispersion model developed by [62] can be adopted, as follows:

$$R_t = \left(\frac{4}{3}\right)^{0.75} \cdot {c_E}^{0.5} \left(\frac{\rho}{2\pi}\right)^{0.25} \cdot V^{0.25} t^{0.75} \tag{3}$$

where R_t is the radius of the area in which cloud might be ignited at time t; c_E is an empirical constant approximately equal to 1; V is the volume flow rate of the flammable gas; ρ is the vapor density relative to air. This dispersion model is suitable for low-wind conditions and neglects the effects of obstacles on dispersion.

2.2.2. Numbering hazardous installations

$M = [1, 2, 3, \ldots, m]$ is a set of nodes representing the hazardous installations that may be involved in the evolution of hazards.

2.2.3. Numbering human positions

$N = [m + 1, m + 2, m + 3, \ldots, m + n]$ is a set of nodes denoting the human position that may be affected by toxic release, fire, or overpressure hazards.

2.2.4. Numbering ignition sources

$K = [m + n + 1, m + n + 2, m + n + 3, \ldots, m + n + k]$ is a set of nodes denoting the ignition sources that may cause the ignition of a flammable vapor cloud.

2.2.5. Node states

S is a node parameter indicating the state of installations, humans and ignition sources at the evolution time *T*. According to possible major hazards in industrial areas and the vulnerability characteristics of hazardous installations and humans, five states of hazardous installations, three human states, and three states of ignition sources are defined, as shown in Tables 1–3. As shown in Table 1, the state of "operational" is an initial state while the state of "extinguished" is a terminal state. The states of "release", "fire" and "VCE" are harmful to other installations and humans. If a release occurs at an installation, the state of the installation changes from "operational" to "release". The state of "fire" is caused by an immediate ignition while the state of "VCE" results from delayed ignition. Table 2 shows human states including one initial state "safe" and two terminal states "injured" and "dead". Table 3 lists the four states of ignition sources, including one initial state (inactive), one terminal state (ignited) and one intermediate state (ignited). It should be noted that all the foregoing states are time-dependent and may be updated with the spatial-temporal evolution of the hazards.

2.2.6. Physical effects

E is a set of directed edges denoting the physical effects that may cause damage to hazardous installations or be harmful to humans. In this study, the heat radiation induced by fire, the overpressure caused by VCEs and the toxicity induced by toxic vapor are considered. There are six kinds of directed edges: the heat radiation from installation nodes to installation nodes or human nodes, the overpressure from installation nodes to installation nodes or human nodes, and the toxic effects from installation nodes to human nodes or ignition nodes.

2.2.7. Acute intoxication

C is a set of edge parameters from release source to human denoting the concentration of toxic vapor at human positions. The acute intoxication of exposed humans caused by a toxic cloud depends on the toxic concentration (C_t) and exposure time (t_e). The probit function for acute intoxication is used to quantify the death probability due to human exposure to toxic vapor, as follows:

$$Y_t = c_1 + c_2 \ln(C_t^{c_3} \times t_e) \tag{4}$$

where c_1, c_2 and c_3 are constants that vary with different toxic substances. These constants for different toxic substances can be adopted from the Green Book [63]. Y_h is the probit value of human vulnerability exposure to toxic gas. Aa a result, the death probability (f_t) caused by acute toxicity can be obtained using Eq. (5):

$$f_t = \phi(Y_t - 5) \tag{5}$$

ϕ is the cumulative distribution function of the standard normal distribution. It should be remarked that besides the toxic concentration and exposure time, other factors such as demographics (e.g. ages) and Personal Protection Equipment (PPE) are not considered in this formula.

Table 1
States of hazardous installations.

State	Description
Operational	The hazardous installation is not physically damaged and is operational.
Release	The hazardous installation is physically damaged, resulting in the loss of containment of hazardous materials and/or poisoning humans nearby.
Fire	The installation is on fire due to immediate ignition, causing heat radiation on humans and/or other installations.
VCE	The installation's loss of containment induces a vapor cloud explosion due to delayed ignition.
Extinguished	The installation is physically damaged but does not generate any hazardous effects.

Table 2
States of humans.

State	Description
Safe	The human does not receive any hazardous effects.
Injured	The human is injured due to exposure to toxic gas, heat radiation, or overpressure.
Dead	The human is decreased due to exposure to toxic gas, heat radiation, or overpressure.

Table 3
States of ignition sources.

State	Description
Inactive	Flammable vapor is not present at the ignition source, or the concentration of the vapor is out of the flammability limit.
Active	Flammable materials are present at the ignition source, and the concentration of the vapor is between the lower and upper flammability limits.
Ignited	The ignition source has ignited the flammable vapor.

2.2.8. Damage induced by VCEs

P is an edge parameter denoting the overpressure generated by VCEs when the flammable vapor is ignited by an ignition source. The commonly-used overpressure estimation methods include the TNT equivalent method, the Baker-Strehlow method and CFD simulation, etc. The TNT equivalent method is a simple approach based on TNT explosion mechanism to calculate overpressure, which neglects the effects of space configuration, ignition sources and flammable gas distribution and thus may underestimate the overpressure. The Multi-Energy method is developed for gas explosions, dividing the explosion as a number of sub-explosions and addressing the effects of congestion levels, ignition and gas distribution in obstructed areas. Netherlands Organization for Applied Scientific Research (TNO) recommended the Multi-Energy method for overpressure calculation in quantitative risk analysis [61]. Consequently, the Multi-Energy method [62] is adopted to calculate the overpressure *P* obtained by different installations and humans. According to this method, the overpressure induced by VCEs depends on the strength coefficient (c_s) and the scaled distance (r_s). The c_s is a constant parameter (1–10) determined by the congestion of the chemical plant. In view of the severe consequences caused by past VCE accidents in chemical industrial areas, the most conservative value of 10 is usually assigned to c_s in risk assessment [48]. The scaled distance r_s is characterized by four parameters: the mass of the flammable vapor (M_f), the combustion heat of the vapor (ΔH) and the distance between the calculation point (installations or humans) and the explosion center (r), as shown in Eq. (6):

$$r_s = \frac{r}{\left(M_f \times \Delta H / P_a\right)^{1/3}} \tag{6}$$

Then the overpressure obtained by different installations and humans can be derived from a blast chart [64]. The damage probability of hazardous installations and death probability caused by overpressure (f_p) can also be calculated by the application of probit functions, as follows:

$$Y_p = c_4 + c_5 \ln(P) \tag{7}$$

where c_4 and c_5 are constants, as shown in Table 4.

Table 4
Probit function parameters of different installations and human exposure to overpressure.

Installations	Atmospheric	Pressurized	Elongated	Auxiliary	Human
c_4	−9.36	−14.44	−12.22	−12.42	−77.1
c_5	1.43	1.82	1.65	1.64	6.91

The damage probability of installations or the death probability of humans induced by overpressure is calculated by the application of Eq. (7) while substituting Y_p for Y_t.

2.2.9. Damage induced by fires

H is a $m \times (m+n)$ matrix representing the heat radiations generated by nodes in "fire" states. $h_{i,j}$ is an element of the matrix denoting the heat radiation induced by an installation i in a "fire" state to installation or human j, as follows:

$$H = \begin{bmatrix} 0 & h_{1,2} & \cdots & h_{1,m+n} \\ h_{1,2} & 0 & \cdots & h_{2,m+n} \\ \cdots & h_{i,j} & 0 & \cdots \\ h_{m,1} & \cdots & h_{m,m+n-1} & h_{m,m+n} \end{bmatrix} \tag{8}$$

H is not a square matrix because people can only receive but not generate heat radiation. Considering possible synergistic effects [8] induced by multiple installations in the "fire" states, the heat radiation received by a node j (Q_j) can be calculated as:

$$Q_j = \sum_{i=1}^{m} h_{i,j} \tag{9}$$

Considering that installation i starts receiving effective heat radiation at evolution time t_g, the residual failure time $T_{f_i}^{t_g}$ of the installation can be calculated as [65]:

$$T_{f_i}^{t_g} = \frac{\exp(c_6 \times V^{c_7} + c_8 \ln(Q_i^{t_g}) + c_9)}{60} \tag{10}$$

where $T_{f_i}^{t_g}$ is the residual failure time of installation i at t_g (min); The values of c_6, c_7, c_8, and c_9 are shown in Table 5.

If the received heat radiation Q_{i,t_g} evolves to $Q_{i,T_{g+1}}$ at $t = t_{g+1}$ and the $T_{f_i}^{t_g} > t_{g+1} - t_g$, the installation i will not be physically damaged at t_{g+1}, and the residual time to failure of installation i in the "heat up" state at the time t_{g+1} will be updated according to the superimposed effect model [41].

$$T_{f_i}^{t_{g+1}} = \left(\frac{Q_i^{t_{g+1}}}{Q_i^{t_g}}\right)^c \times \left(T_{f_i}^{t_g} - t_{g+1} + t_g\right) \tag{11}$$

The vulnerability of humans exposed to heat radiation is estimated by using the exposure time and the received heat radiation (Q). Consequently, the probit value of human vulnerability exposure to multiple fires can be estimated as:

$$Y_f = -14.9 + 2.56\ln\left(6 \times 10^{-3} \times Q^{1.33} \times T_e\right) \tag{12}$$

The heat radiation received by people (Q) varies with the number of hazardous installations in the "fire" state during the spatial-temporal evolution of hazards. Therefore, the hazardous effects caused by heat radiation on humans at different time periods should be superimposed (e.g., the superimposed effects of heat radiation on human vulnerability). At evolution time t_G, the probit value ($Y_f^{t_G}$) can be estimated as:

$$Y_f^{t_G} = -14.9 + 2.56\ln\left(6 \times 10^{-3} \times \sum_{g=1}^{g=G} \left(Q_g^{1.33} \times t_g\right)\right) \tag{13}$$

Finally, the death probability (P_f) can be calculated by the cumulative distribution function ϕ in Eq. (5).

During fire escalation, emergency response measures such as firefighting may effectively extinguish the fires and thus prevent the evolution of hazards. Thus a cumulative log-normal distribution function is adopted to model the uncertainty of the time needed for an effective emergency (t_e) [8]:

$$\log t_e \sim N(u, \sigma^2) \tag{14}$$

u is the mean value, and σ^2 is the variance of log t_e.

Table 5
The values of c_6, c_7, c_8, and c_9 [65].

Installation	c_6	c_7	c_8	c_9
Atmospheric tank	-2.67×10^{-5}	1	−1.13	9.9
Pressurized tank	8.845	0.032	−0.95	0

2.2. Graph update rules

Fig. 1 shows the state transitions and physical effects due to different states in HEGs. As shown in Fig. 1, Dotted lines represent state transition of nodes and solid line denote physical effects caused by a node to other nodes. Humans may be injured due to acute toxicity caused by installations in the "release" state, heat radiation induced by installations in the "fire" state, as well as overpressure caused by installations in the "VCE" state. Since human vulnerability to heat radiation and toxic vapor depends on the intensity of the physical effects and the exposure time, humans may die after a period time of exposure. But the overpressure induced by VCEs may induce an immediate death since the death likelihood caused by explosions is determined by the intensity of explosion regardless of the exposure time. In a hazard evolution caused by overfilling, a human may suffer from different hazards at different subsequent times.

To further illustrate the graph update rules, Fig. 2 shows an example of a HEG with 9 static graphs. As shown in Fig. 2, a hazardous installation's state changes from "operational" to "toxic release" when a toxic release occurs at the installation (e.g., T1 in Fig. 2a) due to accidental events, natural events, or intentional attacks. If the released material is ignited immediately, the installation's state will change to "fire" and induce heat radiation on humans and other hazardous installations. Otherwise, a vapor cloud may form and disperse along with the vaporization of the release material, resulting in acute toxicity, as shown in Fig. 2b.

As the vapor cloud continues to spread, the ignition source may change from an "inactive" state to an "active" state (Fig. 2c). As a result, a VCE may occur when the vapor cloud is ignited, resulting in the damage of hazardous installations and casualties. As shown in Fig. 2d, T2 and T4 are damaged by the VCE while T3 is not. At time t_4, both H1 and H2 become exposed to the overpressure caused by the VCE but the injury of H1 may be more severe than that of H2 since the former suffers from acute toxicity as well. Simultaneously, T2 and T4 may be on fire because the explosion can release a lot of heat and energy which increases the likelihood of immediate ignition at the two damaged tanks. As shown in Fig. 2e, the two tanks in "fire" states induce synergistic effects of heat radiations on H1, H2, and T3. H1 may die at time t_5 (Fig. 2f) while H2 may die at time t_6 (Fig. 2g). The state of T4 changes from "fire" to "extinguished" at t_5 due to the burn out of flammable substances. Finally, the fire at T2 is extinguished and T3 survives since the escalation is blocked by firefighting actions. The evolution ends since there is no escalation.

2.3. Simulation algorithm

Fig. 2 uses a dynamic graph to represent an evolution process of hazards originating from a toxic release. Evolution uncertainties such as the ignition time and the death probability of humans cannot be fully considered by listing all the possible hazard evolution paths. Besides, the evolution may be more complex when it comes to real chemical storage areas with multiple ignition sources and many hazardous installations. As a result, Monte Carlo simulation is employed to generate DHEGs, addressing the time-dependencies and uncertainties in the hazard evolution process. Fig. 3 shows the developed algorithm based on the HEG model and the Monte Carlo simulation.

According to the simulation algorithm, at first, basic data is inputted, including the number of iterations (NI_{max}), the industrial layout, release

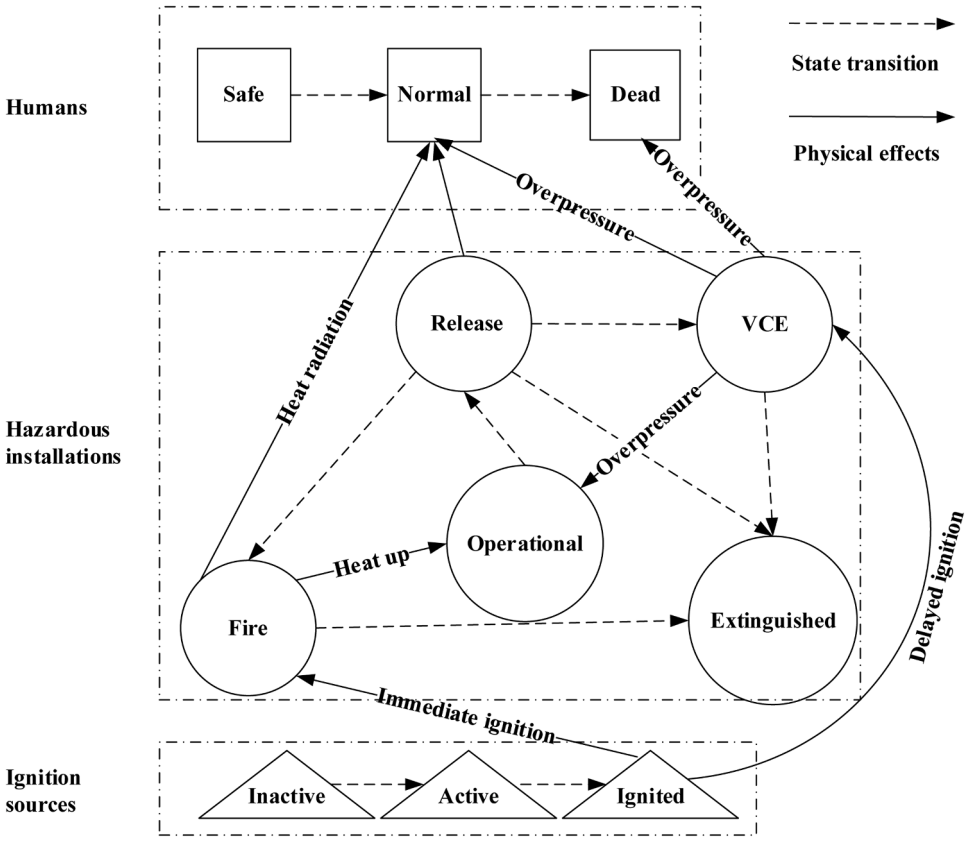

Fig. 1. State transition and physical effects causing the transition among different states.

scenarios, possible ignition sources, etc. Next the ignition type is determined by random sampling. If it is a delayed ignition, the ignition time (*IT*) and the ignition source are determined by random sampling based on Eq. (2). Death caused by toxic vapors can also be determined using Eq. (4). At the *IT*, the HEG updates and the curves in the graph represent overpressure. The overpressures suffered by humans and hazardous installations can be calculated based on Eq. (6). As a result, the fatalities and the subsequent fires caused by the overpressure can be obtained by random sampling based on Eq. (7). The graph will be updated again at the *IT*, and the curves in the graph will then represent heat radiation. The heat radiation can be calculated by the application of ALOHA, and then the time to failure of hazardous installations can be determined using Eqs. (10) and (11). If there is an immediate ignition, the calculation procedures for explosion and toxic vapor are neglected, and the heat radiation is immediately calculated. During the fire escalation period, the graph is updated when a new fire occurs, or an existing fire is extinguished when the evolution is over.

The above calculations are repeated $NI_{\max}$ times. Finally, the death probability and failure probability of installations during the dynamic hazardous evolution are obtained. Besides, the possible evolution paths, evolution time nodes, expected DIT can also be determined using the simulation.

3. Application of the methodology

The DGMC methodology consisting of the HEG model and the simulation algorithm was developed in Section 2. To demonstrate its application to a dynamic hazard evolution, an illustrative case study is used in this section.

3.1. Case study

A chemical storage facility including 37 chemical storage tanks (T1-T37) in three tank areas (I, II, III), 5 possible human positions (H1-H5), and two possible ignition sources (S1-S2) is considered in this study. The layout of the chemical storage facility is shown in Fig. 4. Table 6 summarizes the main characteristics of the storage tanks considered in the dynamic vulnerability analysis.

An overfilling of acrylonitrile at T1 with a filling rate of 100 kg/s was considered as the primary scenario. The release of acrylonitrile can result in acute intoxication and the subsequent explosions and fires may lead to human's exposure to overpressure and heat radiation. The released acrylonitrile vaporizes and disperses around. The ambient temperature is 0 °C and the wind speed is equal to zero. According to the vapor cloud dispersion model in Eq. (8), the ignition source S1 is active after 5.1 min while S2 is active after 2.8 min. The autoignition probability P_{ia} is zero and the ignition probability due to static discharge P_{is} is estimated as 0.02 given the minimum ignition energy of 0.16 mJ [66] and the autoignition temperature of 481 °C [67]. The possible heat radiations induced by tanks and the burning rates of fires are calculated through the ALOHA software. The number of iterations (*NImax*) is set as 10^5 in which the computation time is 3.9 min, and the average deviation of two computations is lower than 0.001. In terms of large chemical plants with many installations, the computation time will increase though being still acceptable. Taking the case with 150 tanks [8] as an example, the computation time would be 21 min. This computation is conducted by an ordinary personal computer (Intel (R) Core (TM) i7 CPU, 8GB RAM). The computation time can be deviously reduced by using a computer with better computation performance.

3.2. Results

Due to the spatial-temporal evolution of hazards, humans may get exposed to different hazards. The death probabilities caused by different hazards at H1-H5 are shown in Fig. 5.

As shown in Fig. 5, both the total death probabilities at H1 and H2

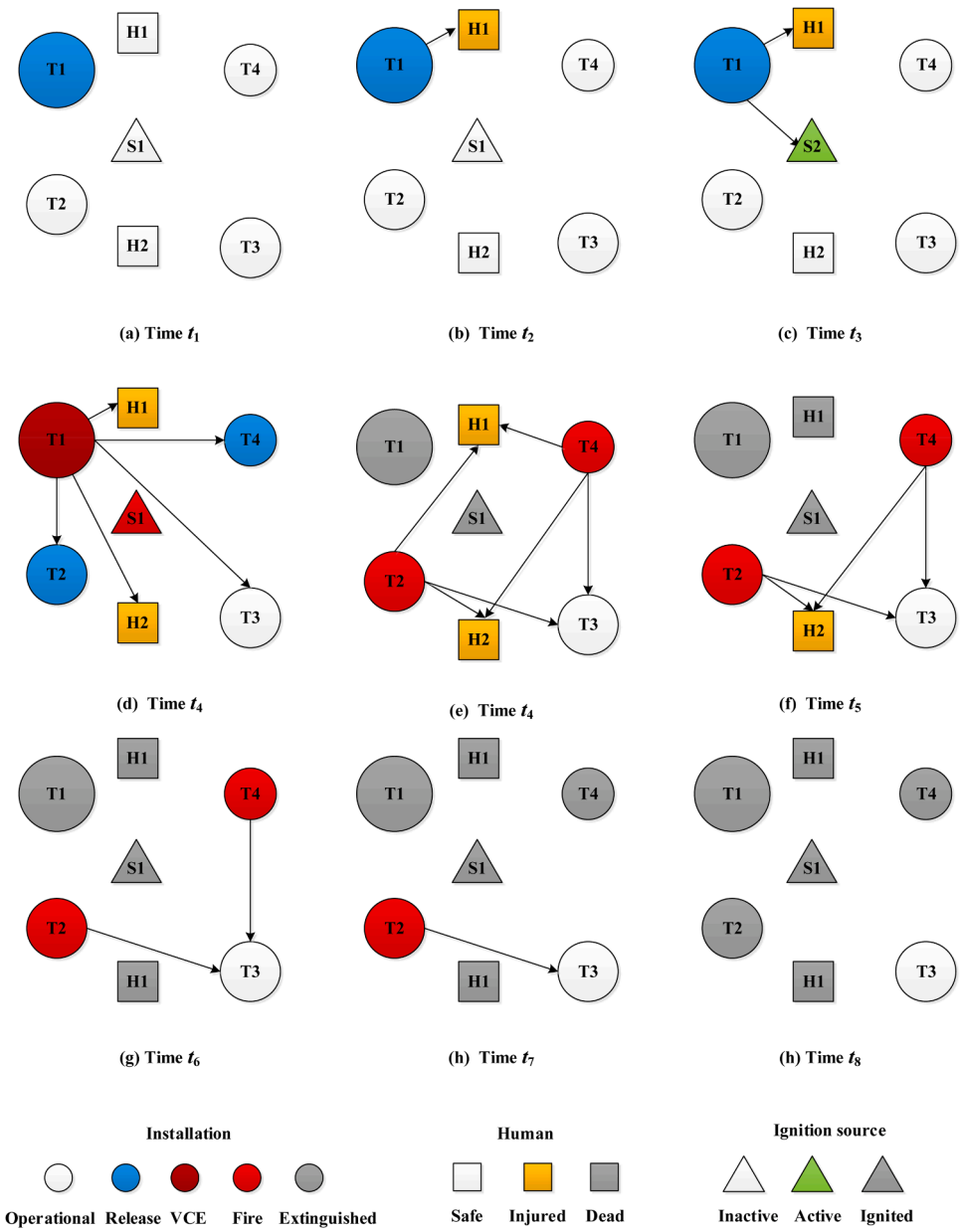

Fig. 2. A HEG with 9 static graphs.

are around 0.99, indicating that people at H1 and H2 will die due to the toxicity and fire. The total death probabilities at H1 and H2 are approximately equal to their death probabilities caused by toxicity or fire. It demonstrates that people at H1 and H2 may simultaneously or sequentially receive multiple hazards. Humans at H1, H4 and H5 are mainly threatened by toxicity and fire while the main hazards at H2 include toxicity, VCE, and fire. The hazards at H3 are dominated by toxicity since it is far from T1, and it is not in the storage tank area. Although there is a long distance between T1 and H5, fire can escalate from tanks nearby T1 to the tanks close to H5. The results can be explained by analyzing the spatial-temporal evolution between the hazards. In this case, explosion is not the main cause of fatalities, but it can cause injures such as eardrum rupture. The probability of eardrum rupture at H1 and H2 is 0.34 and 0.68, respectively. According to these results, different kinds of PPEs can be assigned to humans in different positions. For example, humans at H3 only need to take a gas mask while protective clothing to protect against potential heat is also needed for humans at H1, H2, H4 and H5 due to possible multi-hazard. More details of PPE are presented in the Discussion.

Fig. 6 shows the failure probabilities caused by fires and explosions of the 27 hazardous tanks due to the overfilling of acrylonitrile at T1. The failure probabilities of T1-T6 in tank area I is around 0.98 since they are close to the release source. The failure probabilities of tanks in storage area II obviously decrease with increasing the distance between the release sources and the tanks (e.g., T7-T11, T12-T15). The failure probabilities of tanks in tank area III are much lower than those of the tanks in storage areas I and II since they are located farther from the release source T1. Besides, the fires cannot escalate from area II to area III due to the safety distance between these areas. However, the explosion at tank areas I and II can damage the tanks in area III, possibly resulting in fires. It indicates that the safety distances provided for preventing fire escalation is not sufficient to prevent the damage caused by VCEs.

The tanks around T1 (i.e., T1-T8 and T12) are more likely to be directly damaged by explosions (VCEs). These damaged tanks may result in multiple fires, and the fires may escalate spatially as well as

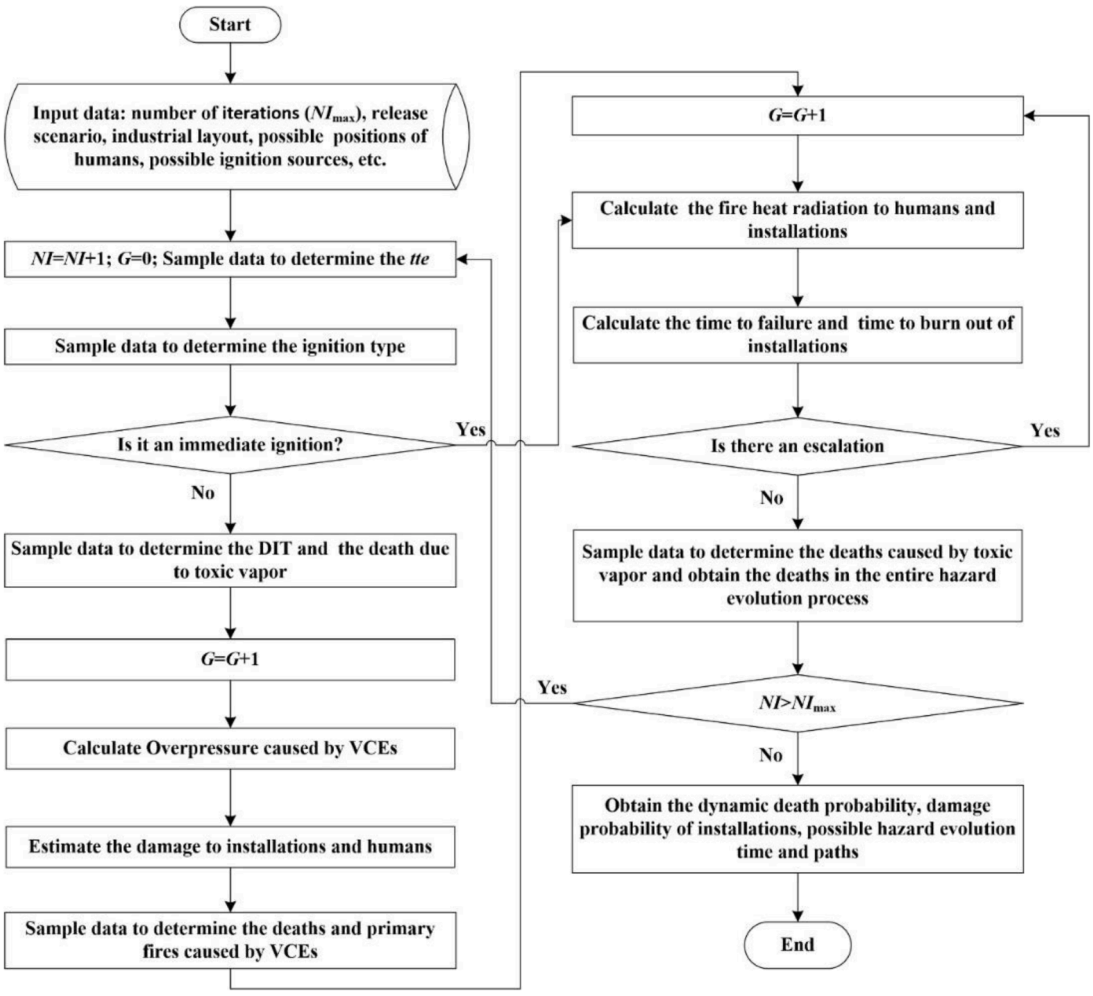

Fig. 3. Simulation algorithm for the HEG model.

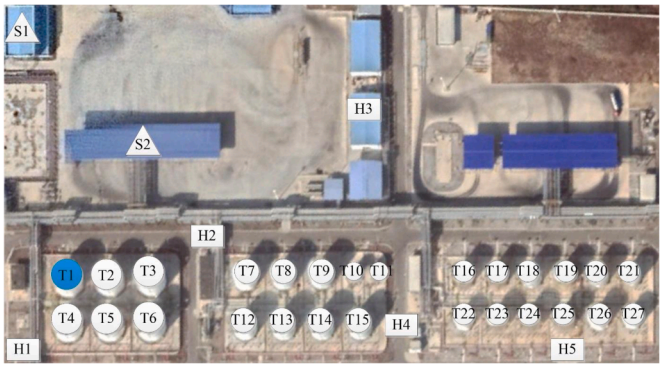

Fig. 4. Chemical storage facility considered in the case study.

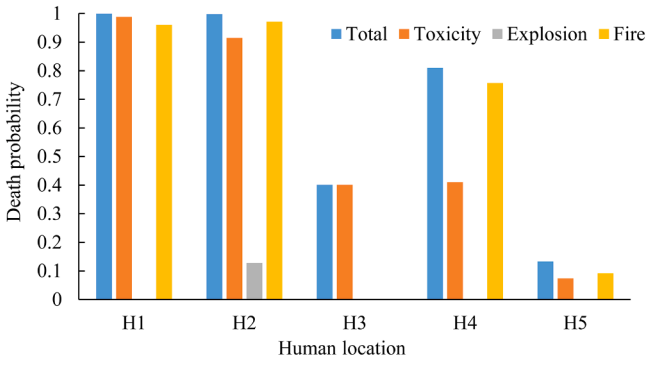

Fig. 5. Death probabilities caused by different hazards at H1-H5.

Table 6
Characteristics of chemical storage tanks.

Tank	Type	Dimension × Height (m)	Chemical substance	Nominal volume (m^3)	Chemical content (m^3)
T1-T6	Atmospheric	21.0 × 16.6	Acrylonitrile	5000	4000
T7-T9, T12-T15	Atmospheric	17.0 × 15.4	Gasoline	3000	2400
T10, T11	Atmospheric	7.0 × 13.6	Gasoline	500	400
T16-T27	Atmospheric	14.5 × 12.7	Gasoline	2000	1600

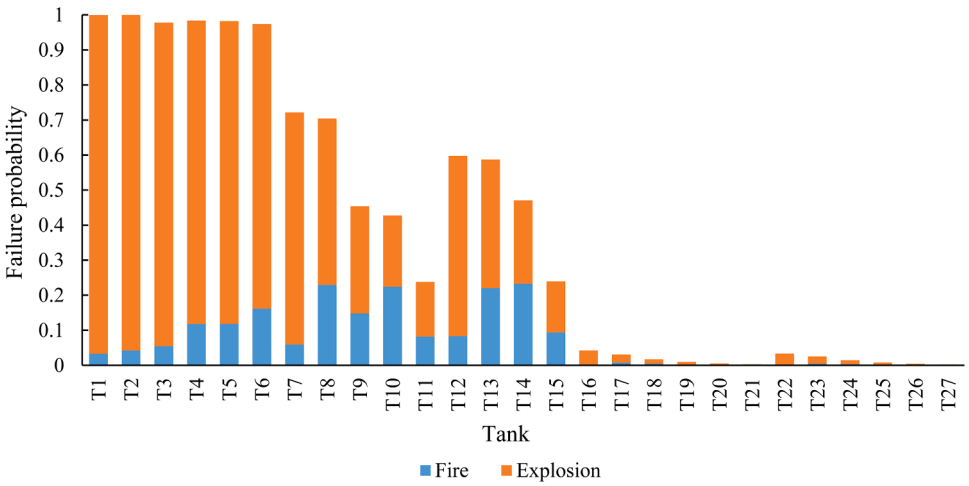

Fig. 6. Failure probabilities of tanks caused by fire and explosion.

temporally, resulting in the damage of other tanks such as T10 and T11. Fig. 7 exemplifies one of the possible hazard evolutions: acrylonitrile starts releasing from T1 at $t = 0$; the released acrylonitrile forms a flammable vapor cloud, and the vapor cloud disperses around. People at H1 and H2 get exposed to the toxic gas at $t = 1.3$ min and $t = 3.0$ min, respectively. The ignition source S2 is active at $t = 2.8$ min while S2 is active at $T = 5.1$ min. Then the vapor cloud is ignited by S2 at $t = 7.6$ min, resulting in a VCE. During the vapor dispersion process, people at H1 and H2 die due to acute toxicity. At $t = 7.6$ min, 11 tanks (T1-T9, T11, T12, and T15) are damaged and catch fire due to the overpressure caused by the VCE. The fires rapidly escalate to T10, T13 and T14. Finally, people at H4 die due to heat radiation.

As shown in Fig. 7, T10, T13 and T14 are damaged by multiple fires at $t = 10.4$ min due to synergistic effects. The result demonstrates that fire escalation after a delayed VCE is usually inevitable. Despite the fact that the fire cannot escalate from tank storage area II to tank storage area III due to the physical distance between them, there is a low probability for the tanks in storage area III to get damaged (0.0–0.1) and for people at H5 to die (0.09) in a fire: This case may happen if a VCE causes damage to the tanks in the storage area III and subsequently triggers fire in the area. It indicates that the tanks are more vulnerable to VCEs and the safety distances solely based on fire risk assessment would be ineffective for VCEs.

Due to the hazard evolution, the death probabilities of humans at H1, H2 and H4 change over time. Fig. 8 shows the cumulative probabilities of death at H1, H2, and H4. People at H1 start inhaling toxic vapor at $t = 1.3$ min when the toxic vapor spreads to H1 and the death probabilities increase over time due to the amount of inhaled toxic vapor. The cumulative probability of death at H2 increases from $t = 3.0$ min when the people at H2 when people at H2 begin to be exposed to toxic gas. At $t = 7.6$ min, multiple tank fires are induced by the VCE, resulting in hazardous effects at H1, H2 and H4. As a result, the cumulative probability of death at H4 starts to increase due to the induced heat radiation and that at H1 and H4 further increase due to toxicity and heat radiation.

4. Discussion

The case study in Section 3 demonstrates that multi-hazard chemicals (e.g., acrylonitrile) in the process industry can simultaneously or sequentially lead to multiple hazards to humans and installations due to the cascading effects. The results are consistent with the characteristics of the disaster in Zhangjiakou, China (2019). Based on the case study, this section discusses parameters that may have considerable effects on human vulnerability and the multi-hazard evolution.

4.1. Atmosphere parameters

Atmosphere parameters such as ambient temperature and wind have an impact on the evaporation of liquid hazardous materials and the dispersion of vapor clouds. Both wind speed and direction have been shown to affect the vulnerability of humans and facilities during cascading effects [41]. Since large disasters caused by overfilling usually occur at low wind conditions [68], only the effects of temperature on the death probability of humans and the failure of hazardous tanks are discussed in this study. As shown in Fig. 9, both the death probability of humans and the failure probability of tanks increase with the rise of ambient temperature. As shown in Fig. 9a, the death probability of humans at H3 only slightly increases with rising temperature, indicating that acute toxicity is not sensitive to temperature. The reason is that the rise of ambient temperature increases the toxic gas concentration while decreases the delayed ignition time (DIT). The failure probabilities of tanks in tank area III (T16-T27) are much lower than those in area II since the physical distance between tank area II and III becomes a barrier for fire escalation between the two areas. When the ambient temperature rises, the likelihood of tank failure in tank area III increases rapidly since the overpressure caused by VCEs increases so does the damage likelihood of tanks in area III. In general, humans with lower death probabilities and tanks with lower failure probabilities are more sensitive to ambient temperature. It can be demonstrated that the damage effects increases with increasing ambient temperature.

4.2. Flow rate

The flow rate is a key parameter for characterizing a loss of containment. Since the amount of hazardous material released is proportional to the flow rate, the death probability increases with increasing flow rate, as shown in Fig. 10a. The death probability at the five positions slightly rises with the increase of flow rate. Fig. 10b shows the effects of flow rate on the failure probabilities of hazardous tanks. All the failure probabilities of the 27 tanks display an increasing trend when increasing the flow rate. Therefore, it can be demonstrated that a larger release is more likely to result in more severe consequences, no matter what hazards the release causes. By comparing Fig. 10 with Fig. 9, it can be demonstrated that the effect of flow rate is much smaller than that of ambient temperature since the evaporation rate of toxic vapor is more sensitive to ambient temperature than the flow rate. For example, the concentration of toxic vapor increase by 34% if the flow rate increases from 80 kg/s to 160 kg/s while that increases by 170% when the ambient temperature increases from 20 °C to 40 °C.

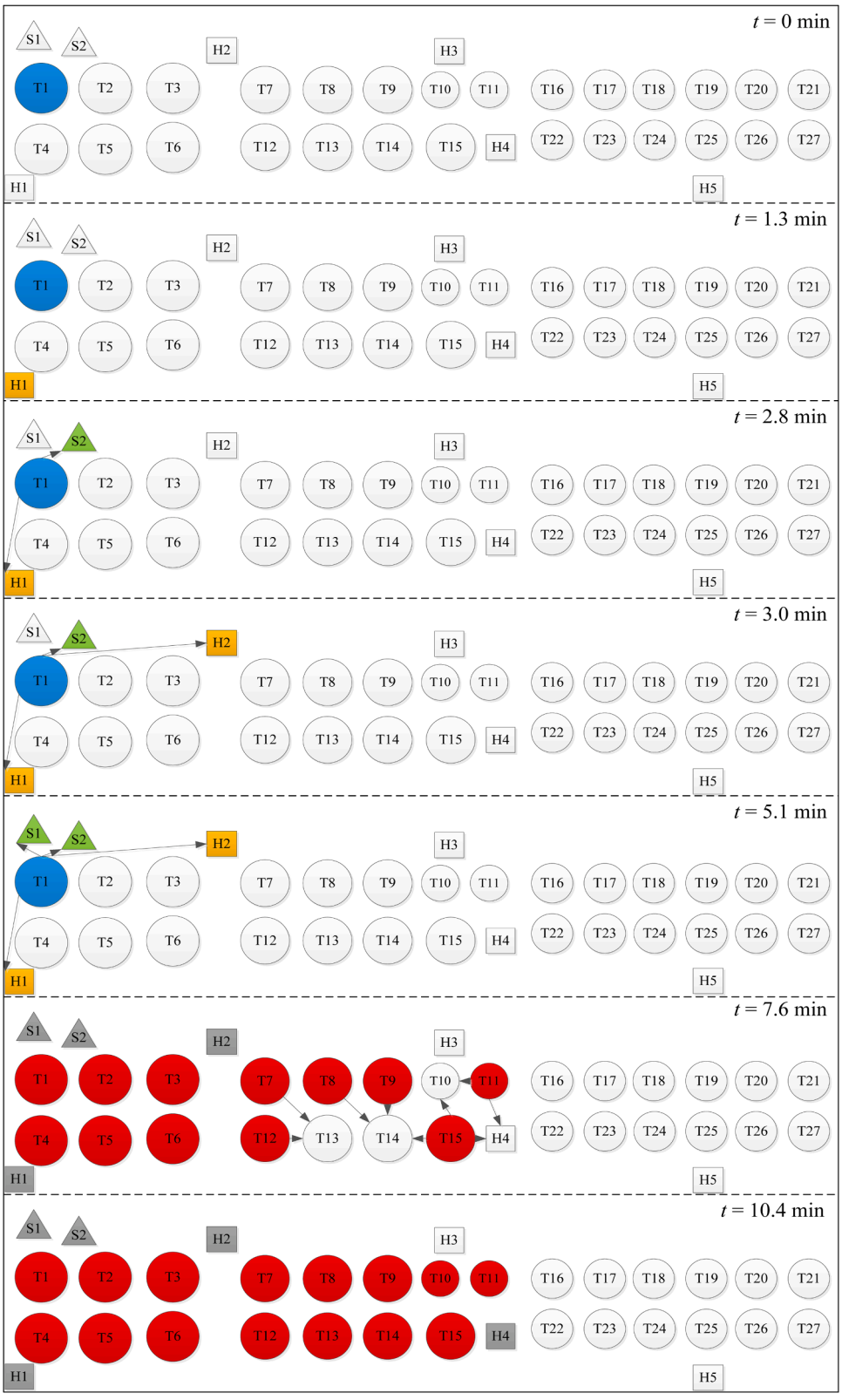

Fig. 7. One of the hazard evolution processes including toxic release, VCE and fire.

4.3. Probability of immediate ignition

An immediate ignition can lead to fire but the increase of the probability of immediate ignition (PII) decreases the likelihood of VCEs and toxicity. Fig. 11 illustrates the effects of FII on the total death probability of humans and the total failure probability of the tanks. Both the death probability and failure probability decrease with an increase of the PII. It indicates that the damage caused by the fire is lower than the damage caused by VCEs and toxicity. The total risk caused by hazardous materials towards individuals and facilities may be underestimated if only

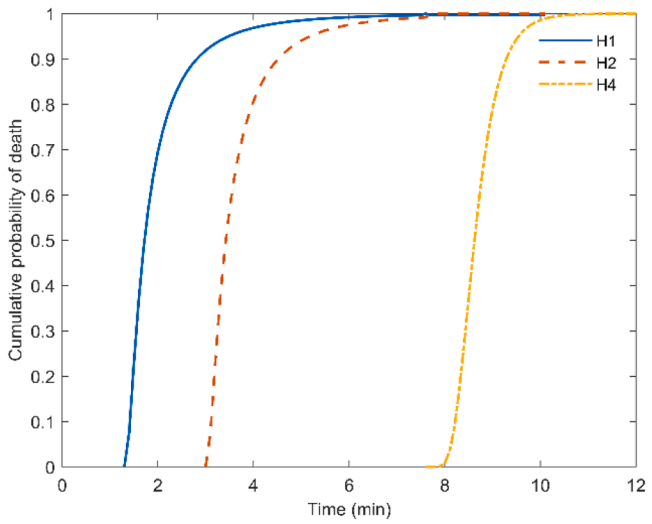

Fig. 8. The cumulative probabilities of death at different positions.

fire hazard is considered in the hazard evolution. The tanks close to the release source are more sensitive to the PII because an increase of PII sharply decreases the damage probability caused by VCEs, as shown in Fig. 11b.

4.4. Emergency response

The time needed for effective emergency response (t_e) is essential for mitigating the consequences of a disaster by cutting or delaying the spatial-temporal escalation of hazards. In this study, a log-normal distribution is used to model the uncertainty of t_e. The effects of the average values of t_e (μ) on the total death probability and failure probability are shown in Fig. 12. As shown in Fig. 12a, The death probability of humans far from the release source increases with increasing the time needed for emergency response while the death probability at H1 and H2 close to the release source is not sensitive to the t_e. It is more difficult to rescue people near the release source via emergency response. The failure probability of tanks also increases with the increase of tee. Besides, tanks are more vulnerable to fire are more likely to survive since the emergency response can largely decrease the possibility of fire escalation.

4.5. Personal protection equipment

PPE is used to minimize human exposure to hazards, such as respirators, protective clothing, helmets, goggles, glasses and other garments that are designed to prevent the wearer from hazards [69]. In the case study, the main hazards for humans are toxic gas and heat radiation. Respirators are commonly used for protecting humans from toxicity by filtering out toxic gases in the air [70]. In case PPE is available in chemical plants, a human response time of 5 s for humans to respond to hazardous scenarios is considered [63]. Fig. 13 shows the death probabilities of humans with respirators in different positions. Compared to Fig. 5 (without respirators), the death probability caused by acute intoxication is largely reduced. For example, the death probability at H1 decreases from 0.99 to 0.05, decreasing by 95%. However, the total death probabilities at H1, H2 and H4 don't decrease since people at these positions are also threatened by heat radiation. As a result, thermal protective clothing is needed to provided enough time for humans to escape from fire scenarios [63,71]. Fig. 14 shows the death probabilities under the protection of respirators and thermal protective clothing.

As shown in Fig. 14, the total death probabilities at H1-H5 are decreased due to the application of respirators and thermal protective clothing. In the case scenario, both respirators and thermal protective clothing are needed for people at H1, H2, H4 and H5 while only respirators are needed in H3 since people may only be exposed to toxic hazards. Consequently, this study can facilitate the allocation of PPE for

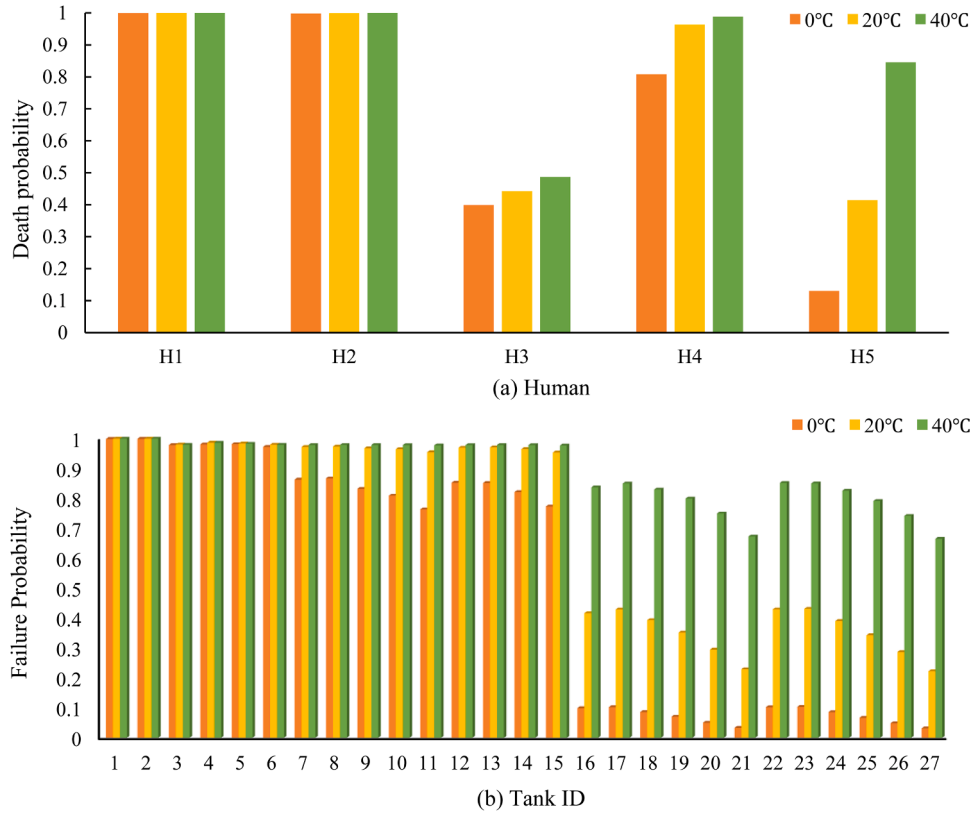

Fig. 9. The effects of ambient temperature on (a) the total death probability of humans, and (b) the total failure probability of installations.

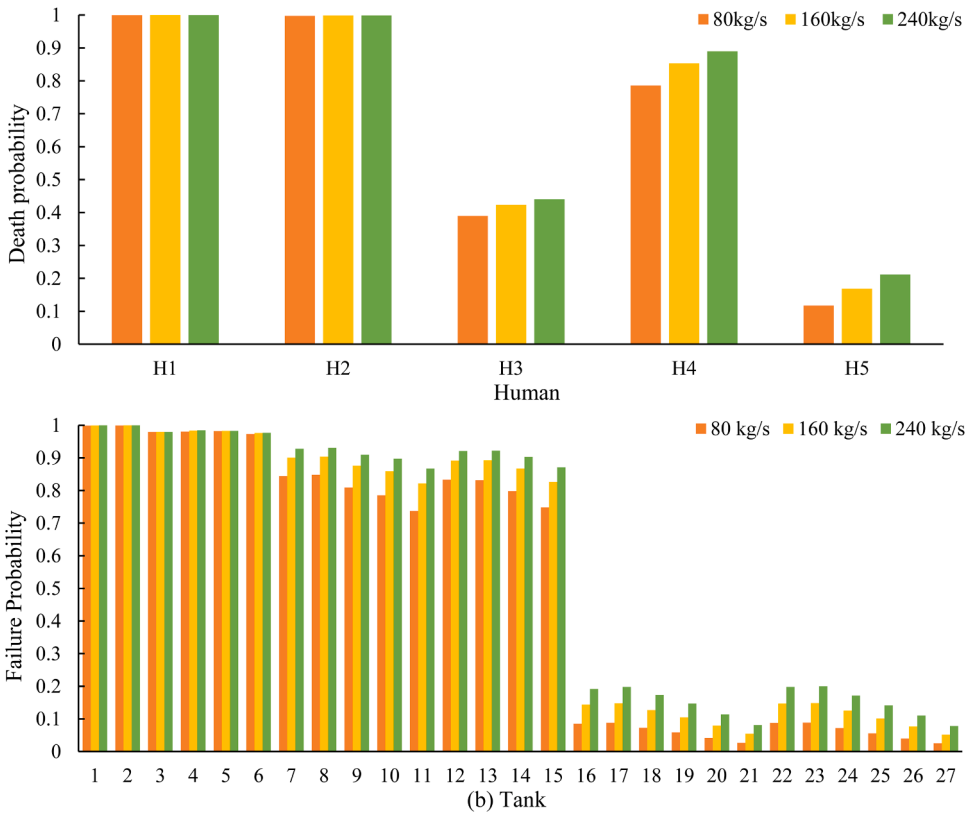

Fig. 10. The effects of flow rate (F) on (a) the total death probability of humans and (b) the total failure probability of tanks.

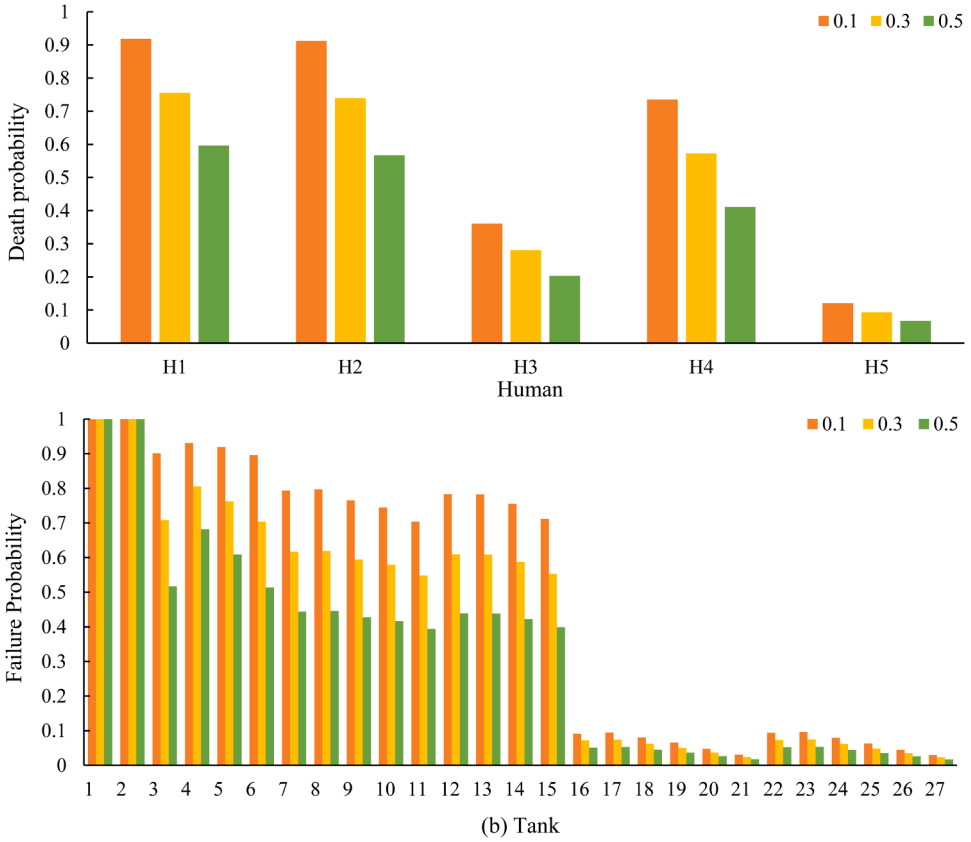

Fig. 11. The effects of the probability of immediate ignition (PII) on (a) the total death probability and (b) the total failure probability.

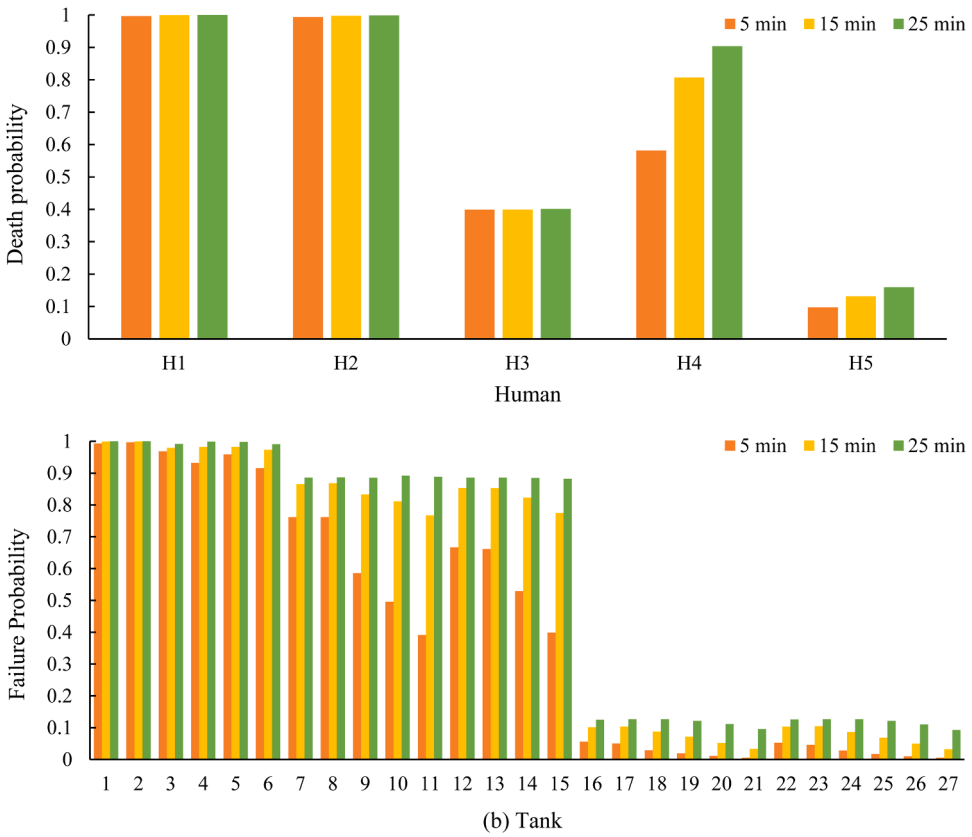

Fig. 12. The effects of emergency response parameter μ on (a) the total death probability of humans and (b) the total failure probability of tanks.

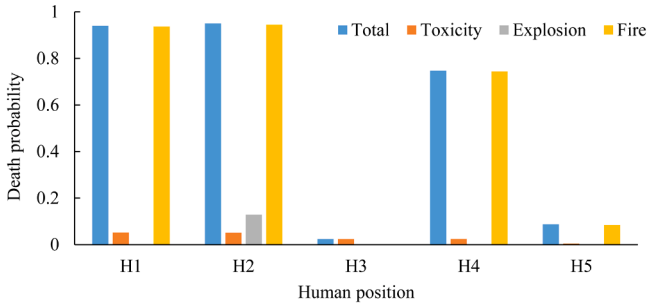

Fig. 13. The effects of respirators on the death probabilities at different positions.

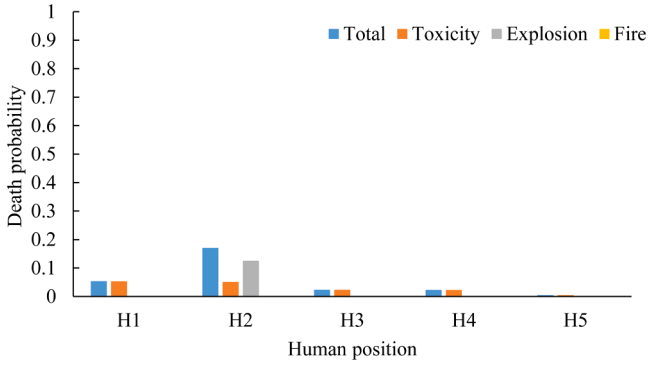

Fig. 14. The effects of respirators and thermal protective clothing on the death probabilities at different positions.

people at different positions and avoid underestimating hazards and unreasonable allocation of protection resources.

Besides the discussed issues, in the future, CFD [72] may be used to model the dispersion of toxic gas, considering the influences of wind velocity and obstacles on dispersion, thus improving the accuracy of the proposed method. In terms of Monte Carlo simulation, the application of more advanced computers may be needed for the case with hundreds of installations and multiple ignition sources.

5. Conclusions

There are many installations for storage, transport, or process of hazardous materials in chemical process plants. Once a release occurs at an installation, hazards as toxic release, VCE and fire can simultaneously or sequentially occur, and the generated hazards can evolve spatially and result in a cascading disaster.

In this study, a dynamic methodology based on dynamic graphs and Monte Carlo simulation is developed to assess the vulnerability of humans and facilities in exposure to multiple hazards while considering the spatial-temporal evolution of the hazards. A case study was used to illustrate the application of the methodology and its capabilities in modeling the occurrence and evolution of time-dependent multi-hazard under uncertainty.

The main achievements of the present study can be summarized as follows: (i) The methodology can effectively model simultaneous and sequential multiple hazards caused by the release of hazardous materials; (ii) only considering one type of hazard in vulnerability assessment may largely underestimate the risk, possibly resulting in ineffective allocation of personal protection equipment (PPE); (iii) humans in different locations may be threatened by different hazards, thus different protection strategies may be formulated for people within and around the chemical plants; (iv) VCE and toxic release may result in more severe consequences than fire as long-delayed ignition can result

in the damage of multiple installations and acute toxicity of people around the release source; (v) the concurrent fires resulting from a VCE may be inevitable due to a rapid escalation rate and limited emergency resources; (vi) hazardous installations are more vulnerable to VCEs, and the safety distances based on fire hazards are not sufficient for VCEs; (vii) people close to the release source are prone to multi-hazards while the deaths outside the hazardous storage areas are mainly caused by acute toxicity and VCEs.

CRediT authorship contribution statement

Chao Chen: Methodology, Data curation, Writing - original draft. **Genserik Reniers:** Conceptualization, Supervision, Writing - review & editing. **Nima Khakzad:** Visualization, Resources, Writing - review & editing.

Declaration of Competing Interest

The authors declare that they have no known competing for financial interests or personal relationships that could have appeared to influence the work reported in this paper.

References

[1] Reniers G, Cozzani V. Domino effects in the process industries, modeling, prevention and managing. Amsterdam, The Netherlands: Elsevier; 2013.
[2] Khan F, Rathnayaka S, Ahmed S. Methods and models in process safety and risk management: past, present and future. Process Saf Environ Prot 2015;98:116–47.
[3] Reniers GLL, Audenaert A. Preparing for major terrorist attacks against chemical clusters: intelligently planning protection measures w.r.t. domino effects. Process Saf Environ Prot 2014;92(6):583–9.
[4] Wu J, Zhou R, Xu S, Wu Z. Probabilistic analysis of natural gas pipeline network accident based on Bayesian network. J Loss Prev Process Ind 2017;46:126–36. https://doi.org/10.1016/j.jlp.2017.01.025.
[5] Wang B, Wu C. Safety informatics as a new, promising and sustainable area of safety science in the information age. J Clean Prod 2020;252.
[6] Yang Y, Chen G, Reniers G, Goerlandt F. A bibliometric analysis of process safety research in China: understanding safety research progress as a basis for making China's chemical industry more sustainable. J Clean Prod 2020;263.
[7] Ge W, Sun H, Zhang H, Li Z, Guo X, Wang X, et al. Economic risk criteria for dams considering the relative level of economy and industrial economic contribution. Sci Total Environ 2020;725.
[8] Chen C, Reniers G, Khakzad N. Integrating safety and security resources to protect chemical industrial parks from man-made domino effects: a dynamic graph approach. Reliab Eng Syst Saf 2019;191.
[9] Wang B, Li D, Wu C. Characteristics of hazardous chemical accidents during hot season in China from 1989 to 2019: a statistical investigation. Saf Sci 2020;129.
[10] Yang Y, Chen G, Reniers G. Vulnerability assessment of atmospheric storage tanks to floods based on logistic regression. Reliab Eng Syst Saf 2019:106721.
[11] Wang B, Wu C, Reniers G, Huang L, Kang L, Zhang L. The future of hazardous chemical safety in China: opportunities, problems, challenges and tasks. Sci Total Environ 2018;643:1–11.
[12] Vilchez JA, Sevilla S, Montiel H, Casal J. Historical analysis of accidents in chemical plants and in the transportation of hazardous materials. J Loss Prev Process Ind 1995;8(2):87–96.
[13] CBS. 2015. Final investigation report CARIBBEAN petroleum tank terminal explosion and multiple tank fires. Retrieved from https://www.csb.gov/assets/1/17/06.09.2015_final_capeco_draft_report_for_board_vote.pdf?15462 (Accessed September 20, 2020).
[14] The accident investigation team for "11.28" accident. The investigation report of "11.28" large explosion-fire accident of Shenghua Chemical Company. Zhangjiakou China Chemical Industry Group; 2019. Retrieved from, http://www.xinhuanet.com/energy/2019-05/24/c_1124535295.htm (Accessed June 13, 2020).
[15] Zhou J, Reniers G. Petri-net based evaluation of emergency response actions for preventing domino effects triggered by fire. J Loss Prev Process Ind 2018;51:94–101.
[16] Zhou J, Reniers G. Probabilistic Petri-net addition enabling decision making depending on situational change: the case of emergency response to fuel tank farm fire. Reliab Eng Syst Saf 2020;200.
[17] Georgiadou PS, Papazoglou IA, Kiranoudis CT, Markatos NC. Modeling emergency evacuation for major hazard industrial sites. Reliab Eng Syst Saf 2007;92(10):1388–402.
[18] Olivar OJR, Mayorga SZ, Giraldo FM, Sánchez-Silva M, Pinelli J-P, Salzano E. The effects of extreme winds on atmospheric storage tanks. Reliab Eng Syst Saf 2020;195.
[19] Misuri A, Casson Moreno V, Quddus N, Cozzani V. Lessons learnt from the impact of hurricane Harvey on the chemical and process industry. Reliab Eng Syst Saf 2019;190.
[20] Chen G, Huang K, Zou M, Yang Y, Dong H. A methodology for quantitative vulnerability assessment of coupled multi-hazard in Chemical Industrial Park. J Loss Prev Process Ind 2019;58:30–41.
[21] Chen C, Reniers G, Khakzad N. A thorough classification and discussion of approaches for modeling and managing domino effects in the process industries. Saf Sci 2020;125. https://doi.org/10.1016/j.ssci.2020.104618.
[22] Li Z, Li W, Ge W. Weight analysis of influencing factors of dam break risk consequences. Nat Hazards Earth Syst Sci 2018;18(12).
[23] Mishra KB, Wehrstedt K-D, Krebs H. Lessons learned from recent fuel storage fires. Fuel Process Technol 2013;107:166–72.
[24] Mishra KB, Wehrstedt K-D, Krebs H. Amuay refinery disaster: the aftermaths and challenges ahead. Fuel Process Technol 2014;119:198–203.
[25] Maremonti M, Russo G, Salzano E, Tufano V. Post-accident analysis of vapour cloud explosions in fuel storage areas. Process Saf Environ Prot 1999;77(6):360–5.
[26] Taveau J. The Buncefield explosion: were the resulting overpressures really unforeseeable? Process Saf Prog 2012;31(1):55–71.
[27] Sharma RK, Gurjar BR, Wate SR, Ghuge SP, Agrawal R. Assessment of an accidental vapour cloud explosion: lessons from the Indian Oil Corporation Ltd. accident at Jaipur, India. J Loss Prev Process Ind 2013;26(1):82–90.
[28] Dasgotra A, Varun Teja GVV, Sharma A, Mishra KB. CFD modeling of large-scale flammable cloud dispersion using FLACS. J Loss Prev Process Ind 2018;56:531–6.
[29] Mishra KB. The influence of volume blockage ratio on IOCL Jaipur explosion. J Loss Prev Process Ind 2018;54:196–205.
[30] Gant SE, Atkinson GT. Dispersion of the vapour cloud in the Buncefield Incident. Process Saf Environ Prot 2011;89(6):391–403.
[31] Salzano E, Cozzani V. The use of probit functions in the quantitative risk assessment of domino accidents caused by overpressure. Leiden: A a Balkema Publishers; 2003.
[32] Cozzani V, Salzano E. The quantitative assessment of domino effects caused by overpressure: part I. Probit models. J Hazard Mater 2004;107(3):67–80.
[33] Cozzani V, Salzano E. The quantitative assessment of domino effect caused by overpressure: part II. Case studies. J Hazard Mater 2004;107(3):81–94.
[34] Zhang M, Jiang J. An improved probit method for assessment of domino effect to chemical process equipment caused by overpressure. J Hazard Mater 2008;158(2–3):280–6.
[35] Mukhim ED, Abbasi T, Tauseef SM, Abbasi SA. Domino effect in chemical process industries triggered by overpressure—formulation of equipment-specific probits. Process Saf Environ Prot 2017;106:263–73.
[36] Zhou J, Reniers G. Petri-net based cascading effect analysis of vapor cloud explosions. J Loss Prev Process Ind 2017;48:118–25.
[37] Yang Y, Chen G, Chen P. The probability prediction method of domino effect triggered by lightning in chemical tank farm. Process Saf Environ Prot 2018;116:106–14.
[38] Khakzad N, Landucci G, Reniers G. Application of graph theory to cost-effective fire protection of chemical plants during domino effects. Risk Anal 2017;37(9):1652–67.
[39] Khakzad N, Reniers G, Abbassi R, Khan F. Vulnerability analysis of process plants subject to domino effects. Reliab Eng Syst Saf 2016;154:127–36.
[40] Khakzad N. Application of dynamic Bayesian network to risk analysis of domino effects in chemical infrastructures. Reliab Eng Syst Saf 2015;138:263–72.
[41] Chen C, Reniers G, Zhang L. An innovative methodology for quickly modeling the spatial-temporal evolution of domino accidents triggered by fire. J Loss Prev Process Ind 2018;54:312–24.
[42] Kamil MZ, Taleb-Berrouane M, Khan F, Ahmed S. Dynamic domino effect risk assessment using Petri-nets. Process Saf Environ Prot 2019;124:308–16.
[43] Zeng T, Chen G, Yang Y, Chen P, Reniers G. Developing an advanced dynamic risk analysis method for fire-related domino effects. Process Safety Environ Prot 2019.
[44] Ding L, Ji J, Khan F. Combining uncertainty reasoning and deterministic modeling for risk analysis of fire-induced domino effects. Saf Sci 2020;129.
[45] Abdolhamidzadeh B, Abbasi T, Rashtchian D, Abbasi SA. A new method for assessing domino effect in chemical process industry. J. Hazard. Mater. 2010;182(1–3):416–26.
[46] Dai J, Xu-Hai P, Min H, Ahmed M, Jun-Cheng J. Assessment of tanks vulnerability and domino effect analysis in chemical storage plants. J Loss Prevent Process Ind. 2019.
[47] He Z, Weng W. Synergic effects in the assessment of multi-hazard coupling disasters: fires, explosions, and toxicant leaks. J Hazard Mater.. 2019.
[48] Chen C, Khakzad N, Reniers G. Dynamic vulnerability assessment of process plants with respect to vapor cloud explosions. Reliab Eng Syst Saf 2020:106934. https://doi.org/10.1016/j.ress.2020.106934.
[49] Galbusera L, Trucco P, Giannopoulos G. Modeling interdependencies in multi-sectoral critical infrastructure systems: evolving the DMCI approach. Reliab Eng Syst Saf 2020;203.
[50] Zhang L, Landucci G, Reniers G, Khakzad N, Zhou J. DAMS: a model to assess domino effects by using agent-based modeling and simulation. Risk Anal 2018;38(8):1585–600.
[51] Chen C, Li C, Reniers G, Yang F. Safety and security of oil and gas pipeline transportation: A systematic analysis of research trends and future needs using WoS. J Clean Prod 2021;279:123583. https://doi.org/10.1016/j.jclepro.2020.123583.
[52] Harary F. Graph theory. Reading, MA: Addison-Wesley; 1969.
[53] Jafari S, Ajorlou A, Aghdam AG. Leader localization in multi-agent systems subject to failure: a graph-theoretic approach. Automatica 2011;47(8):1744–50.
[54] Jiang D, Wu, Cheng B, Xue Z, van Gelder PHAJM J. Towards a probabilistic model for estimation of grounding accidents in fluctuating backwater zone of the Three Gorges Reservoir. Reliab Eng Syst Saf 2020.

[55] Rai S, Hu X. Hybrid agent-based and graph-based modeling for building occupancy simulation. In: Proceedings of the 4th ACM international conference of computing for engineering and sciences; 2018. p. 1–12.
[56] Stroeve SH, Blom HA, Bakker GB. Contrasting safety assessments of a runway incursion scenario: event sequence analysis versus multi-agent dynamic risk modelling. Reliab Eng Syst Saf 2013;109:133–49.
[57] Khakzad N, Reniers G. Using graph theory to analyze the vulnerability of process plants in the context of cascading effects. Reliab Eng Syst Saf 2015;143:63–73.
[58] Rubinstein RY, Kroese DP. Simulation and the monte carlo method. John Wiley & Sons; 2016.
[59] Joy DC. Monte Carlo modeling for electron microscopy and microanalysis. Oxford University Press; 1995.
[60] Kuczera G, Parent E. Monte Carlo assessment of parameter uncertainty in conceptual catchment models: the Metropolis algorithm. J Hydrol (Amst) 1998; 211(1–4):69–85.
[61] Uijt de Haag Ale. Guidelines for quantitative risk assessment. The Hague (NL): Committee for the Prevention of Disasters; 1999.
[62] Atkinson G, Coldrick S. Vapour cloud formation: experiments and modelling. Debyshire, UK: Health and Safety Laboratory; 2012.
[63] Van Den Bosh C, Merx W, Jansen C, De Weger D, Reuzel P, Leeuwen D, et al. Methods for the calculation of possible damage (Green book). The Hague (NL): Committee for the Prevention of Disasters; 1989.
[64] Assael MJ, Kakosimos KE. Fires, explosions, and toxic gas dispersions: effects calculation and risk analysis. CRC Press; 2010.
[65] Landucci G, Gubinelli G, Antonioni G, Cozzani V. The assessment of the damage probability of storage tanks in domino events triggered by fire. Accid Anal Prevent 2009;41(6):1206–15.
[66] Haase H. Electrostatic hazards: their evaluation and control. Wiley-VCH; 1977.
[67] Brazdil J.F., 2000. Acrylonitrile. Ullmann's Encyclopedia of Industrial Chemistry.
[68] Atkinson G. Development of heavy vapour clouds in very low wind speeds. J Loss Prev Process Ind 2017;48:162–72.
[69] OSHA. 2019. Personal protective equipment. Retrieved from https://www.osha.gov/Publications/osha3151.pdf (Accessed August 30, 2020).
[70] Greenawald LA, Karwacki CJ, Palya F, Browe MA, Bradley D, Szalajda JV. Conducting an evaluation of CBRN canister protection capabilities against emerging chemical and radiological hazards. J Occup Environ Hyg 2020:1–15.
[71] Guowen S, Paskaluk S, Sati R, Crown EM, Doug Dale J, Ackerman M. Thermal protective performance of protective clothing used for low radiant heat protection. Text Res J 2010;81(3):311–23.
[72] Yuan S, Wu J, Zhang X, Liu W. EnKF-based estimation of natural gas release and dispersion in an underground tunnel. J Loss Prev Process Ind 2019;62:103931. https://doi.org/10.1016/j.jlp.2019.103931.